PCCP

ROYAL SOCIETY OF CHEMISTRY

PAPER

View Article Online
View Journal | View Issue

Check for updates

Cite this: *Phys. Chem. Chem. Phys.*, 2020, **22**, 18911

Al-doped Fe_2O_3 as a support for molybdenum oxide methanol oxidation catalysts†

Michael Bowker, *[ab] Pip Hellier, [ab] Donato Decarolis,[ab] Diego Gianolio,[c] Khaled M. H. Mohammed,[de] Alex Stenner,[d] Thomas Huthwelker[f] and Peter P. Wells [bcd]

We have made high surface area catalysts for the selective oxidation of methanol to formaldehyde. This is done in two ways – (i) by doping haematite with Al ions, to increase the surface area of the material, but which itself is unselective and (ii) by surface coating with Mo which induces high selectivity. Temperature programmed desorption (TPD) of methanol shows little difference in surface chemistry of the doped haematite from the undoped material, with the main products being CO_2 and CO, but shifted to somewhat higher desorption temperature. However, when Mo is dosed onto the haematite surface, the chemistry changes completely to show mainly the selective product, formaldehyde, with no CO_2 production, and this is little changed up to 10% Al loading. But at 15 wt% Al, the chemistry changes to indicate the presence of a strongly acidic function at the surface, with additional dimethyl ether and CO/CO_2 production characteristic of the presence of alumina. Structurally, X-ray diffraction (XRD) shows little change over the range 0–20% Al doping, except for some small lattice contraction, while the surface area increases from around 20 to 100 $m^2\ g^{-1}$. Using X-ray absorption spectroscopy (XAS) it is clear that, at 5% loading, the Al is incorporated into the Fe_2O_3 corundum lattice, which has the same structure as α-alumina. By 10% loading then it appears that the alumina starts to nano-crystallise within the haematite lattice into the γ form. At higher loadings, there is evidence of phase separation into separate Al-doped haematite and γ-alumina. If we add 1 monolayer equivalent of Mo to the surface there is already high selectivity to formaldehyde, but little change in structure, because that monolayer is isolated at the surface. However, when three monolayers equivalent of Mo is added, we then see aluminium molybdate type signatures in the XANES spectra at 5% Al loading and above. These appear to be in a sub-surface layer with Fe molybdate, which we interpret as due to Al substitution into ferric molybdate layers immediately beneath the topmost surface layer of molybdena. It seems like the separate γ-alumina phase is not covered by molybdena and is responsible for the appearance of the acid function products in the TPD.

Received 2nd March 2020,
Accepted 7th May 2020

DOI: 10.1039/d0cp01192d

rsc.li/pccp

Open Access Article. Published on 29 Mays 2020. Downloaded on 6.05.2026 00:28:13.
This article is licensed under a Creative Commons Attribution 3.0 Unported Licence.

Introduction

The effects of doping haematite with small quantities of aluminium have been explored previously, primarily from a mineralogical perspective, although more recently from the viewpoint of MoO_x/Fe_2O_3 catalysts also.[1–6] Al-substitution into Fe_2O_3 is ubiquitous in terrestrial sources of haematite, but importantly the Al incorporates without significantly disrupting the overall haematite structure.[7] There are, however, small changes in structural properties arising from the presence of Al throughout the haematite structure: typically, structural lattice parameters decrease as a function of the lower atomic displacement of Al in comparison to Fe (0.535 A and 0.645 A respectively). This reduction in lattice spacing and the concomitant altering of electrostatic interactions induces a degree of lattice strain throughout the structure, encouraging the growth of smaller crystallites: this in turn affords a greater value of specific surface area.[6] Since catalytic activity is dependent on surface area, increases in surface area are hugely attractive to the catalysis chemist. In the present case the reaction of interest is the selective oxidation of methanol to yield

[a] *Cardiff Catalysis Institute, School of Chemistry, Cardiff University, Cardiff CF10 3AT, UK. E-mail: bowkerm@cardiff.ac.uk*
[b] *UK Catalysis Hub, Research Complex at Harwell, Rutherford Appleton Lab, Harwell, Oxfordshire OX11 0FA, UK*
[c] *Diamond Light Source Ltd, Harwell Science and Innovation Campus, Didcot OX11 0DE, UK*
[d] *School of Chemistry, University of Southampton, Southampton SO17 1BJ, UK*
[e] *Department of Chemistry, Faculty of Science, Sohag University, Sohag, P.O. Box 82524, Egypt*
[f] *Paul Scherrer Institut, 5232 Villigen-PSI, Switzerland*
† Electronic supplementary information (ESI) available. See DOI: 10.1039/d0cp01192d

Open Access Article. Published on 29 May 2020. Downloaded on 6.05.2026 00:28:13.
This article is licensed under a Creative Commons Attribution 3.0 Unported Licence.

formaldehyde, which is carried out industrially[8] at the scale of ~6 M tonnes per y. The catalyst used is iron molybdate, $Fe_2(MoO_4)_3$, with some extra MoO_3 present.[9] We have previously studied this reaction in some detail and have shown that the active and selective surface is dominated by molybdenum,[10–13] and that good mimics of these materials can be made by simply dosing Mo oxide layers onto the surface of haematite.[14–18]

Initial studies of Al-doped haematite have been conducted as support materials in shell-core selective oxidation catalysts.[6] It was found that the incorporation of 5 wt% Al into Fe_2O_3 doubled the surface area of the post-calcination material, while essentially retaining the corundum structure. Subsequently, after adding MoO_x shell layers to the Al-doped Fe_2O_3 and assessing the reactivity of the resulting catalysts, it was determined that the greater surface area of the catalyst reduced the requisite operating temperature of the catalyst by approximately 20 °C.

A fundamental question is, is there a limit to Al loading, beyond which the normal haematite structure cannot incorporate it? So, one of the primary objectives here was to assess just how much Al can be added before this limit is reached. We aimed to establish whether further increases in the surface area can be achieved at higher Al loading, and what effect this has on structure and reactivity, assessed using a variety of methods. In particular we have utilised the soft X-ray capabilities of the Phoenix beamline at the SLS to carry out Al XANES and EXAFS in order to assess the changes in local structure as Al loading increases.

Experimental

Al-doped haematite samples were prepared by co-precipitation of aluminium nitrate and iron nitrate, after which samples were dried and then calcined at 500 °C for 24 hours. MoO_x/Al-doped Fe_2O_3 catalysts were prepared by an analogous method to MoO_x/Fe_2O_3 and VO_x/Fe_2O_3 by incipient wetness impregnation.[14–17] It is essential to consider the additional surface area present in Al-doped Fe_2O_3 (here called HSA Fe_2O_3) before synthesis, as the calculations used to compute the quantity and concentration of Mo precursor must be adjusted to account for the greater absolute quantity of Mo required to produce the same relative ML coverage.

Raman spectroscopy was conducted using a Renishaw inVia Raman microscope with laser irradiation at 830 nm. Data acquisition was optimized at 1% of laser power. Each spectrum is an accumulation of four scans each with 10 seconds exposure time. To better understanding the effect of Al to haematite structure, a multi-peak fitting analysis was performed using a Lorenzian function. Prior to the fitting, spectra were normalized from 0 to 1 and a Shirley background baseline was subtracted.

The PHOENIX beamline at the Swiss Light Source was used to gather Al K-edge XAS data. PHOENIX possesses two measurement ranges, namely 0.8–8.0 keV and 0.4–2.0 keV, which are ideally suited to measurements with soft X-rays.

Four Al loadings were investigated during the experiment at PHOENIX, namely 5 wt%, 10%, 15% and 20% HSA Fe_2O_3, see the ESI† for further details. For each loading, three samples were analysed: one undoped HSA Fe_2O_3 support; one 1 ML MoO_x/HSA Fe_2O_3 catalyst; and one 3 ML MoO_x/HSA Fe_2O_3 catalyst. Each sample was measured simultaneously in two modes, fluorescence and total electron yield (TEY).

Results and discussion

Structural

Since Al-doping boosts the surface area of these materials, we label Al-doped samples of Fe_2O_3 as high surface area (HSA) Fe_2O_3: the weight proportion of Al in a sample is denoted in percentage terms, so 5 wt% Al-doped Fe_2O_3 is labelled 5% HSA Fe_2O_3.

It was previously found that post-calcination surface area could be almost doubled through the addition of 5 wt% Al to a sample of Fe_2O_3, without incurring any detrimental effects on reactivity, either when used *per se* or as a support for a MoO_x shell.[5] The obvious first experiment therefore was to assess whether further surface area enhancements could be obtained from greater quantities of Al in Fe_2O_3. To that end, several HSA Fe_2O_3 samples were prepared – namely 5%, 10%, 15% and 20% HSA Fe_2O_3 and initially analysed by BET and XRD. A clear trend is visible in surface area as a function of Al loading (Table 1), while no perceptible structural changes were seen by XRD (Fig. S2, ESI†): these were corroborated by repeated batches of HSA Fe_2O_3 materials.

Considerable further gains in surface area can be achieved with greater proportions of Al dopants in Fe_2O_3, reaching a zenith for the 15% HSA at 98.3 $m^2\ g^{-1}$, almost a fivefold increase on un-doped post-calcination Fe_2O_3. It was found that, by making several batches of HSA Fe_2O_3 that the surface area values obtained for 15 and 20% HSA Fe_2O_3 varied around 90 $m^2\ g^{-1}$ ± 10%, with 15% always possessing the highest values. So it seems that a maximum is reached by ~15 wt% Al, after which no further significant increases in surface area can be achieved.

Having determined that greater surface area is attainable with Al doping it is interesting to examine any structural changes which may occur in the Fe_2O_3. XRD data obtained from the HSA catalyst reveals only small differences in peak position and peak width from the undoped haematite (see Fig. S2, ESI†). The main peaks are shifted slightly higher in angle, due to the small decrease in lattice parameter and are broadened compared to Fe_2O_3. This broadening is attributed to the smaller

Table 1 BET-derived surface areas as a function of Al loading in Fe_2O_3

Al loading/wt%	Surface area/$m^2\ g^{-1}$
0	20
5	46
10	71
15	98
20	87

This journal is © the Owner Societies 2020

Open Access Article. Published on 29 Mays 2020. Downloaded on 6.05.2026 00:28:13.
This article is licensed under a Creative Commons Attribution 3.0 Unported Licence.

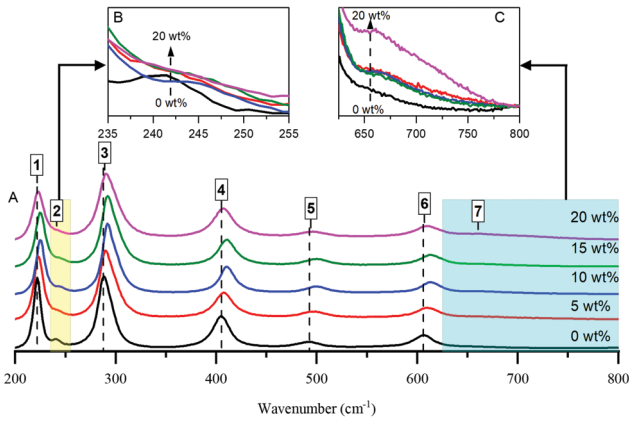

Fig. 1 Raman spectra of Al doped haematite samples (A) with different loadings, as indicated. Spectra are offset vertically for clarity. Inset top graphs represents spectral details in the range of (B) 235–255 cm^{-1} and (C) 625–800 cm^{-1} without any y-offset.

particle size and constrained unit cell growth throughout the Al-doped Fe_2O_3 structures.

The Scherrer equation gives around 22 nm average particle size for post-calcination 15% HSA Fe_2O_3, (the one with the highest surface area) whereas it is ~66 nm for undoped Fe_2O_3. An additional means to determine particle size is by direct imaging, for example, by electron microscopy. Two example images are displayed, for 10 and 15% HSA Fe_2O_3 (Fig. S3, ESI†), which show particles of approximate diameter 40 nm and 25 nm respectively, considerably smaller than for standard Fe_2O_3.

To further examine the effects of Al loading, Raman spectra of the samples were taken and are shown in Fig. 1. Multi-peak fitting using a Lorenzian function analysis was performed. The estimated peak positions and line broadening (FWHM) are summarized in Table S1 (ESI†), in which standard deviations and R square values of each fit are given. Representative examples of the fitting are illustrated in Fig. S4 (ESI†). All of the main Raman bands can be attributed to α-Fe_2O_3.[3,4] There are, however, noteworthy differences in the positions and widths of the peaks, depending on Al content. This can be attributed to the replacement of large numbers of Fe^{3+} cations by smaller Al^{3+} cations, decreasing the separation between cations and therefore boosting the strength of the interconnecting bonds.[3]

The reduction of the band at ~221 cm^{-1} (Fig. 1B) with the development of a shoulder band at ~670 cm^{-1} (Fig. 1C) upon increasing the Al content gives an indication of some perturbation of the α-Fe_2O_3 structure and, by extension, the incorporation of Al cations into the haematite crystal lattice. Moreover, the band at ~405 cm^{-1} of bare haematite, which belongs to O–Fe–O bending modes in $Fe(O)_6$ octahedral geometry, is blue shifted to ~410 cm^{-1} upon increasing Al loading to 15 wt% and thus could be considered as another sign of Al framework contribution. However, the behaviour beyond 15% diverges from the trend: peaks for the 20% HSA Fe_2O_3 sample are less blue-shifted compared to 15% HSA Fe_2O_3. This supports the implication that a plateau is reached by 15% Al, after which further increases in surface area—*i.e.* by reducing particle size—are not feasible.

Reactivity studies of HSA Fe_2O_3

TPD measurements were carried out on the various samples, and examples can be seen in below. The addition of Al to the oxide had little effect on the surface chemistry, with methanol decomposing (*via* the formate surface species[18]) to CO_2 and hydrogen at ~300 °C, Fig. 2. The minor changes were a shifting of the peak to higher temperature by ~20 °C, and a broadening of the peaks, similar to those previously reported by Chapman *et al.*[6] TPD for the four Al loadings are shown in Fig. S5 (ESI†).

After dosing 3 ML of Mo onto the 5 wt% Al doped iron oxide catalyst the desorption pattern is completely changed, Fig. 3. Now we have desorption characteristic of a surface mainly covered by Mo;[11,14–17] the high temperature CO_2 peaks have disappeared and the selective product of methanol oxidation, formaldehyde (30 amu), is seen desorbing at 190 °C, followed by CO (28 amu) with a peak at 225 °C. There are also a number of water desorption peaks (18 amu) the highest being at around 275 °C. This is very similar to the desorption pattern from 3 ML of Mo onto an undoped Fe_2O_3 surface.[14,15] There is very little

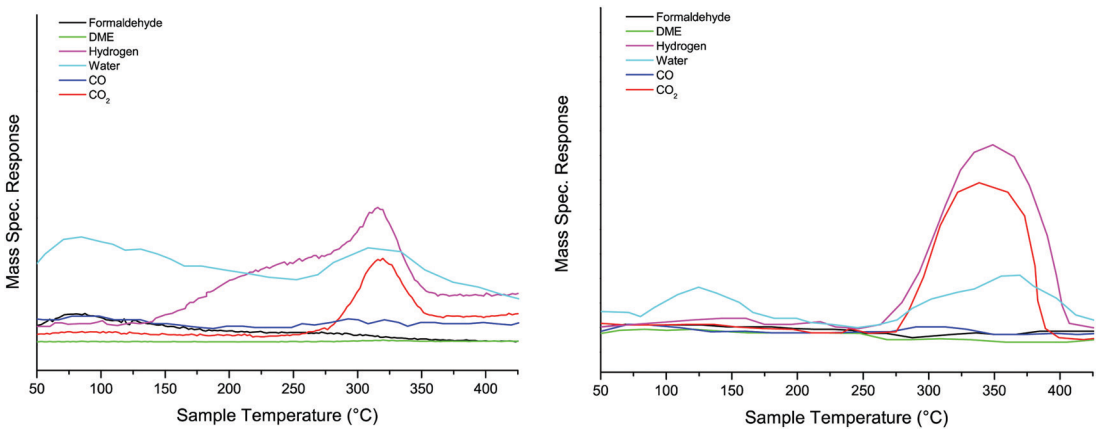

Fig. 2 TPD after dosing methanol on haematite (left panel) and 10% Al doped haematite (right panel).

Open Access Article. Published on 29 Mays 2020. Downloaded on 6.05.2026 00:28:13.
This article is licensed under a Creative Commons Attribution 3.0 Unported Licence.

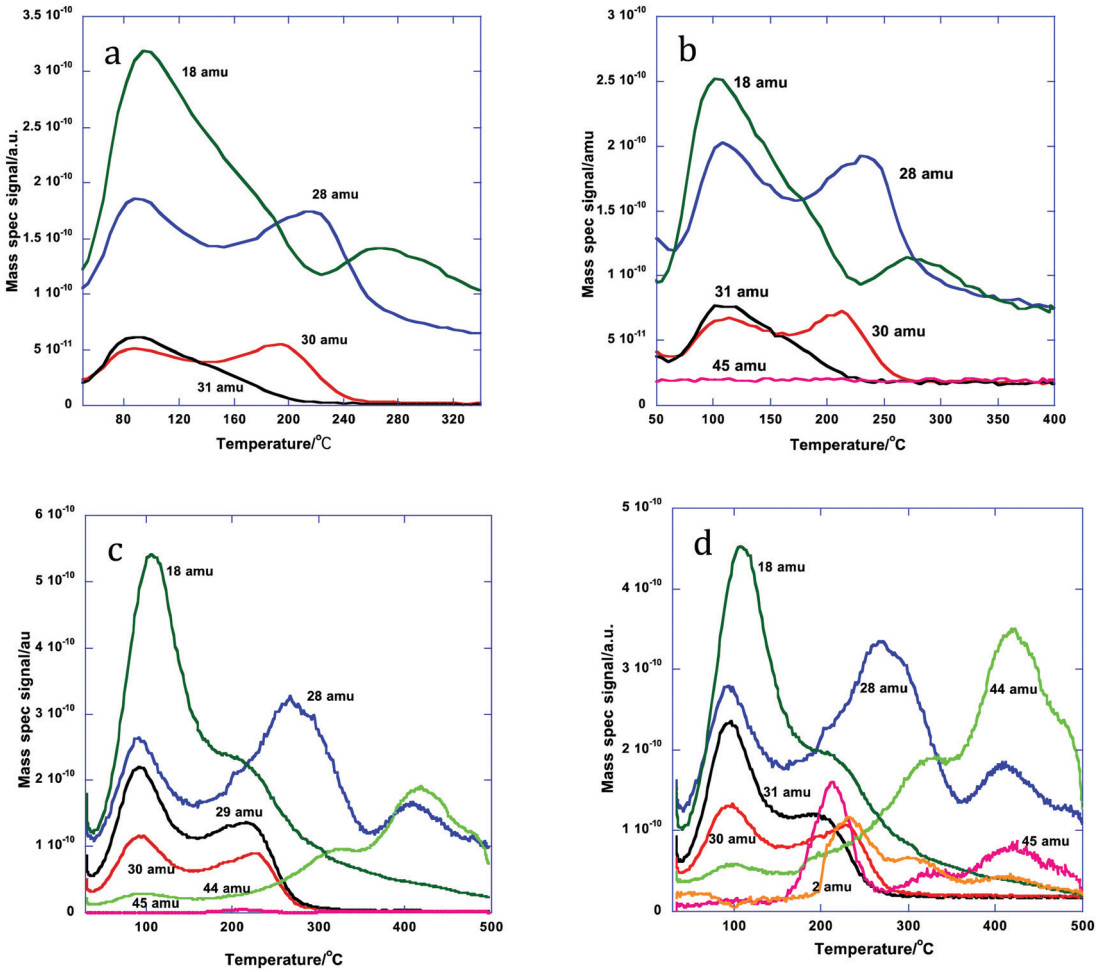

Fig. 3 Desorption products during TPD from the doped HSA Fe_2O_3 samples, coated with 3 ML equivalent of MoO_x: (a) 5% Al doped, (b) 10%, (c) 15% and (d) 20%.

change at 10% loading of Al, except for a small shift in peak temperature for formaldehyde and CO to higher temperature (the latter peaking at ~240 °C). However, the situation changes considerably at 15% loading, with a much bigger ratio of CO to formaldehyde evolution, a further shift and broadening of the CO peak to 280 °C, together with a new CO peak at 400 °C. Additionally there is considerable CO_2 desorption (44 amu) in peaks at 300 and 400 °C, with some signs of dimethyl ether (DME, 45 amu) at 210 °C. These trends continue to 20% Al loading. The DME production is greatly enhanced, as is the CO_2; the DME shows peaks coincident with those of CO_2 at high temperature and the low temperature major peak is at 210 °C. There is also now some hydrogen production in the range from 200 to 500 °C. Thus, at least at loadings up to 10%, the indication is that the surface is little changed by the presence of Al and is essentially covered by Mo, as described in earlier publications,[11,14–17] while at higher loadings there is evidence of the presence of other species present in the material – particularly seen by the peaks of CO, CO_2 and H_2 at around 320 °C and DME at 210 °C. For more detail on identifying these products from the mass spectrometer, see the ESI.†

The changes induced by Mo addition are also shown to a degree by the reactivity data carried out in an oxygen/methanol flow. Fig. 4a below shows that 50% (T_{50}) conversion is achieved at 275 °C for the 15% Al loaded haematite, with CO being formed at low temperature/low conversion, while CO_2 dominates above 20% conversion and reaches near 100% selectivity at high temperature. This is essentially the same result as for undoped haematite. When Mo is dosed onto haematite there is a dramatic change in reaction profile (Fig. 4b), with the dominant product at low temperature being formaldehyde and some DME produced at low temperatures with CO at intermediate temperatures and CO_2 dominating at high temperature (though even there is still some selectivity to H_2CO and CO). The results for Mo dosing onto the Al doped haematite are similar, except for a small shift in conversion to lower temperature as doping increases (due to the increase in surface area), a change to higher CO_2 : CO ratio, and some evidence of DME production at higher temperatures (Fig. 4c). This is the result for 15% Al loading, but the data for all loadings are given in Fig. S6 (ESI†) and Table 2 shows the shift in T_{50} to lower temperature with increased loading, except for the highest, where conversion is reduced somewhat. The selectivities shown

 This journal is © the Owner Societies 2020

Open Access Article. Published on 29 Mays 2020. Downloaded on 6.05.2026 00:28:13.
This article is licensed under a Creative Commons Attribution 3.0 Unported Licence.

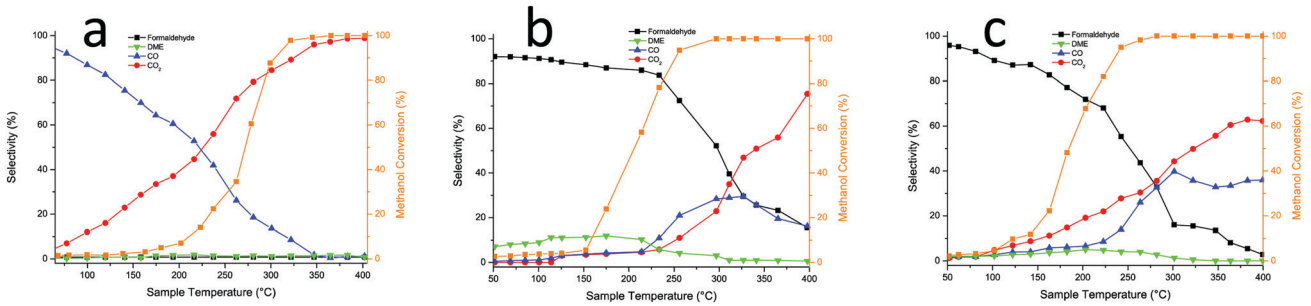

Fig. 4 (a) Reactor results for 15% Al doped Fe_2O_3; (b) for 3 ML Mo on Fe_2O_3; (c) for 3 ML Mo on 15% Al doped Fe_2O_3 catalyst.

Table 2 The effect of Al doping on conversion temperatures for 3 ML Mo on haematite from the ESI in Fig. S6

Catalyst, 3 ML on	T_{50}	T_{100}[a]	S_{50}	S_{100}[a]
Fe_2O_3	205	~300	88	~53
5% Al	195	~280	87	~27
10% Al	190	~275	87	~25
15% Al	185	~280	77	~30
20% Al	200	~290	70	~23

[a] Determined as the first point at which 100% conversion is identified, and the associated selectivity at that point.

in Table 2 at 50% conversion are all high, due to the presence of Mo at the surface, but higher Al loadings result in some detriment to selectivity. The results for these catalysts were unchanged, at least over three sets of runs, and continued running at 250 °C for three hours produced no change in performance within uncertainty limits.

Thus, the big differences seen in anaerobic TPD are not entirely reflected in aerobic reactor studies, but we can say that overall, the surface is Mo dominated and that there appears to be relatively little effect of the Al doping in the bulk up to 10% loading, but some significant changes in the surface chemistry occur above that loading. The changes in the TPD appear to reflect the presence of Al, in some form, at the surface, which provides an acid function to yield DME, and gives decomposition products at high temperature, both of which are also seen on alumina by Akarmazyan *et al.*[19]

Local structure determination using XAS

To probe the Al speciation directly, Al K-edge X-ray absorption spectroscopy was performed and both the X-ray absorption near edge structure (XANES) and extended X-ray absorption fine structure (EXAFS) regions were assessed. Before discussing the spectra of the HSA haematite materials, let us first consider the Al K edge spectra of different phases of alumina (Fig. 5). The pre-edge region of the XANES spectra provides detailed information on the electronic and geometric structures of the Al centre. For α-Al_2O_3 and γ-Al_2O_3 they have characteristic pre-edge features that allow them to be clearly distinguished; α-Al_2O_3 has a single, clearly defined peak in the derivative spectrum at 1560.1 eV, and γ-Al_2O_3 has a broad feature that is resolved as multiple transitions at 1559.6 and 1558.5 eV (Fig. 5b). These features arise as a consequence of Laporte forbidden 1s → 3s transitions, that become partially allowed by the hybridisation of 3s and 3p orbitals as a consequence of non-centrosymmetric coordination centres.[20,21]

When assessing the pre-edge region of the Al doped Fe_2O_3 samples there are additional transitions observed at 1556.2 and 1557.5 eV (Fig. 6a and b). These features arise as a consequence of non-local excitations to the 3d orbitals of neighbouring Fe sites.[22] This is facilitated through the hybridisation with O 2p orbitals that bridge the Al and Fe centres. Two transitions are observed because of the crystal field splitting of the Fe d orbitals into e_g and t_{2g} components; in essence the separation

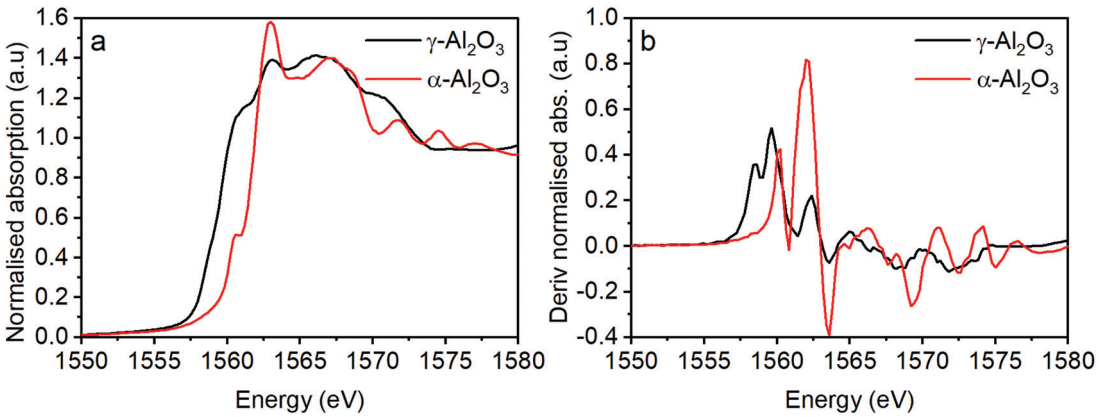

Fig. 5 (a) Al XAS for two morphologies of alumina and (b) the derivatised absorption spectra from (a).

Open Access Article. Published on 29 Mays 2020. Downloaded on 6.05.2026 00:28:13.
This article is licensed under a Creative Commons Attribution 3.0 Unported Licence.

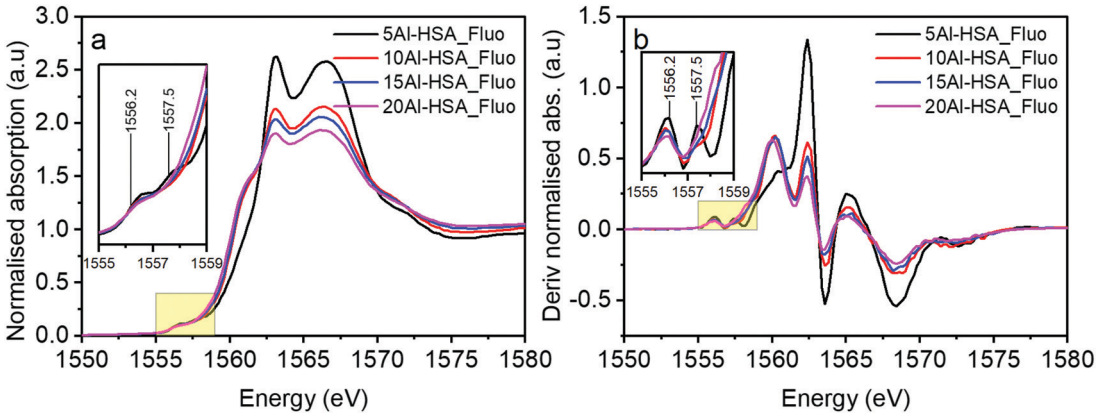

Fig. 6 (a) XAS of Al doped haematite samples taken in fluorescence mode and (b) the derivatised spectra of (a). Inset graphs represent spectra in the range of 1555–1559 eV.

of the peaks is linked to the strength of the crystal field.[23] The relative intensities of these features have previously been ascribed to the extent of Al substitution into a host Fe structure.[4] The differently sized Al^{3+} cation changes the local geometric environment and the extent of Al incorporation affects the Al–O–Fe interactions, *i.e.* this increases with Al content to a certain level, until at which point there is the competition between Al–O–Al and Al–O–Fe interactions. Another significant feature of the HSA samples is the increase in intensity of the transition at 1560 eV (with transitions at similar energies for both alumina reference samples) as a function of increased Al content above 5% loading.

To summarise these findings for Al doping Fig. 7 shows what we believe to be the situation with increasing levels of Al in the sample. First Al units are isolated in the haematite and are isomorphous with the substrate corundum structure. At intermediate loadings these begin to cluster and form nanoclusters, γ-alumina like, within the structure which are too small to be seen by XRD. Finally at the higher loadings separate γ-alumina particles form in the sample, probably precipitated at the surface of the haematite and too small to be seen by XRD.

These Al-doped materials were then coated with Mo. Firstly, we consider the 5% Al HSA sample and compare it with the 1 ML and 3 ML MoO_x modified catalysts (Fig. 8). The MoO_x modification creates core–shell structures where the Mo is concentrated at the surface of the material.[12,14–17] It has previously been established that at 1 ML coverage the Mo remains exclusively at the surface, with additional Mo going on to form sub-surface layers of $Fe_2(MoO_4)_3$. In the case of the 5% Al doped 1 ML MoO_x/Fe_2O_3 the XANES remains largely unchanged compared to the initial 5% doped HSA Fe_2O_3; the Mo is at the surface and not interacting directly with the Al. This observation is consistent with the XANES spectra of the 1 ML MoO_x Al doped Fe_2O_3 samples with increased Al dopant levels (Fig. S7a–c, ESI†).

However, for the 5% Al doped 3 ML MoO_x/Fe_2O_3 there are significant changes to the XANES spectrum (Fig. 8). The major difference is the presence of two pronounced transitions in the pre-edge region at 1557.5 and 1559.0 eV. These peaks are consistent with those found in aluminium molybdate (Fig. 9) and give strong evidence that Al is incorporated into the $Fe_2(MoO_4)_3$ sublayer structure. These transitions have not previously been assigned. However, based on this work, and the arguments above, we propose that they arise from non-local

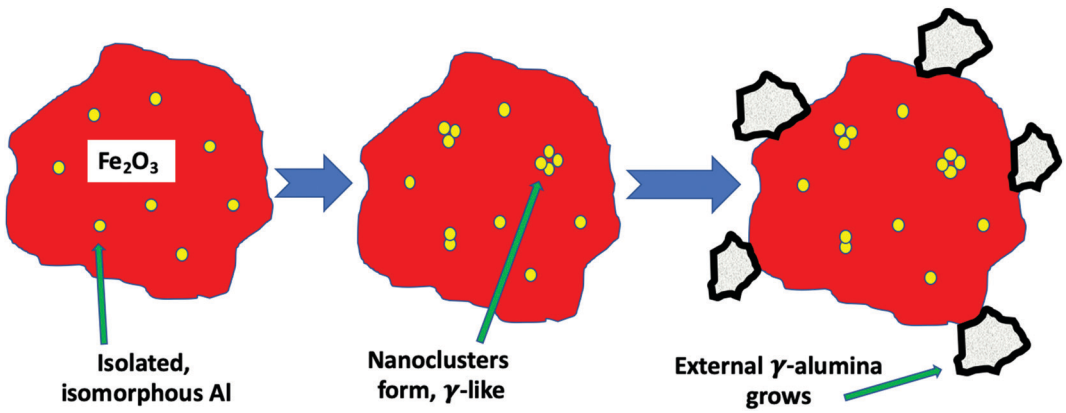

Fig. 7 Showing the evolution of the structure when doping Al into haematite. First the Al is substituted in the lattice with the same corundum structure as the iron oxide. Then small nanoclusters begin to form within the haematite nanoparticles. Finally separated alumina nanocrystals begin to form.

Open Access Article. Published on 29 Mays 2020. Downloaded on 6.05.2026 00:28:13.
This article is licensed under a Creative Commons Attribution 3.0 Unported Licence.

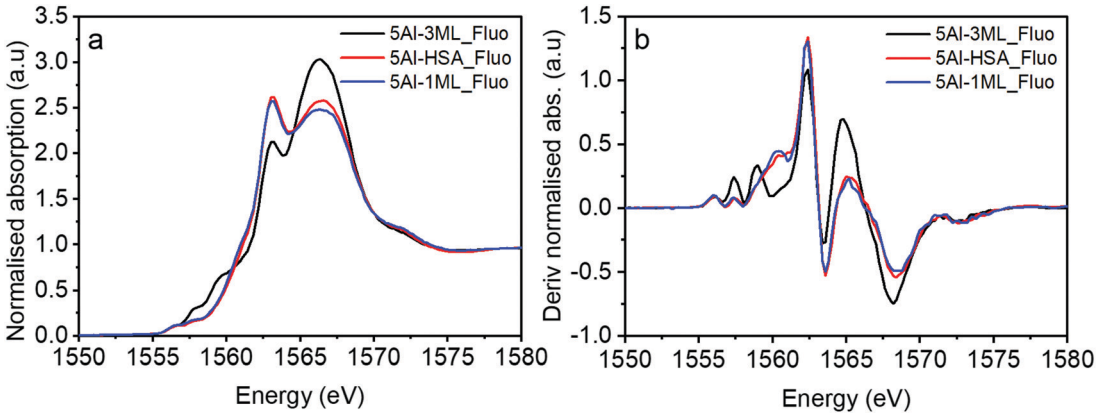

Fig. 8 (a) XAS spectra of the 5% Al haematite sample coated with Mo and (b) its derivative.

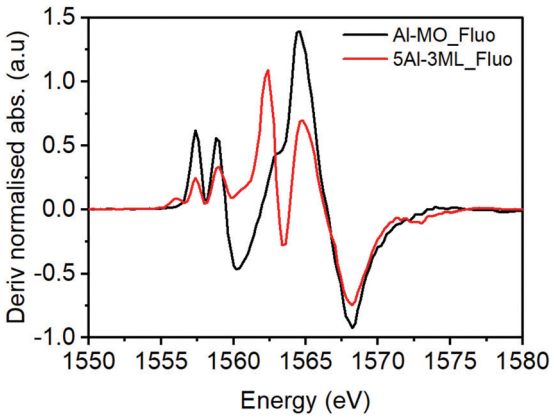

Fig. 9 XAS of the Mo dosed 5% HSA catalyst with an aluminium molybdate reference sample.

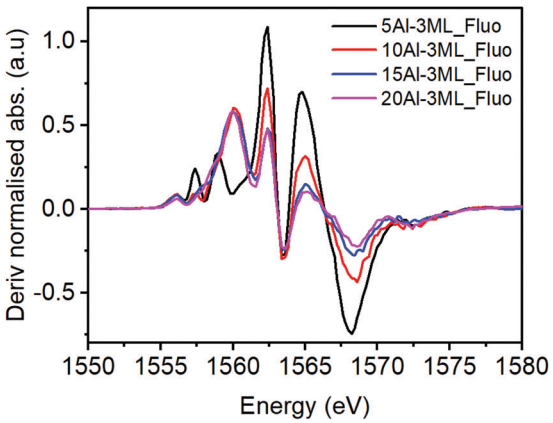

Fig. 10 Derivatised XAS spectra for several loading of HAS catalyst with Mo dosed taken in fluorescence mode.

excitations to Mo 4d states. Considering that the molybdate signature is only found (significantly) in the case of the 5% Al doped 3 ML MoO_x/Fe_2O_3 this would infer that Al is incorporated into an iron molybdate structure. This sample has the most pronounced features for isomorphous substitution. There are other samples where we have evidence for Al segregation (*e.g.* through Raman) and yet there is no evidence of molybdate signatures in these samples despite the potential to create segregated Al molybdate structures.

For the HSA MoO_x/Fe_2O_3 catalysts with higher Al doping (Fig. 10) the molybdate signature disappears and much of the pre-edge region resembles unmodified γ-Al_2O_3. However, the peak at 1557.5 eV for the 10% Al doped 3 ML MoO_x/Fe_2O_3 suggests that there may be some interaction with molybdenum with the higher energy transition being masked by a more intense absorption feature from the γ-Al_2O_3.

Considering the XANES data holistically there are two potential scenarios that we can propose to rationalise our observations: (i) as the Al loading is increased the sample is a mixture of isomorphously substituted haematite and alumina, or (ii) that Al is solely substituted into the haematite lattice. The XANES data is able to confirm the presence of a portion of Al^{3+} within the Fe_2O_3 lattice through the presence of Al 1s to Fe 3d non-local excitations, however, it is only for the 5% Al doped 3 ML MoO_x/Fe_2O_3 catalyst where there is a clear molybdate signature upon MoO_x doping. We assert that this is more consistent with scenario (i) where only a finite amount of Al^{3+} can be inserted into the Fe_2O_3 lattice before phase separation occurs.

Summing up the results obtained from the bare HSA samples, we can say that, at low Al levels, the Al is incorporated into the corundum α-Fe_2O_3 phase substitutionally, with separated Al sites (5% loading). As the Al concentration increases, then a γ-Al_2O_3-like phase is formed as very small units within iron oxide (10%) and, at even higher levels it precipitates out to the surface. When Mo is dosed on the surface at the 1 monolayer level, there is no significant effect on the structure, because it is localised at the surface. However, when higher levels of Mo are present, that in excess of the topmost 1 ML forms subsurface layers of ferric molybdate ($Fe_2(MoO_4)_3$), and when Al is present in the bulk, that is incorporated into the growing subsurface layer to give Al–O–Mo units similar to aluminium molybdate. The effects of Al presence on reactivity are not evident up to 10% loading, indicating that none is present at the surface, while at 15% and above, the reactivity changes to reflect the presence of Al at the surface. These changes include dimethyl ether production at low temperature

Open Access Article. Published on 29 Mays 2020. Downloaded on 6.05.2026 00:28:13.
This article is licensed under a Creative Commons Attribution 3.0 Unported Licence.

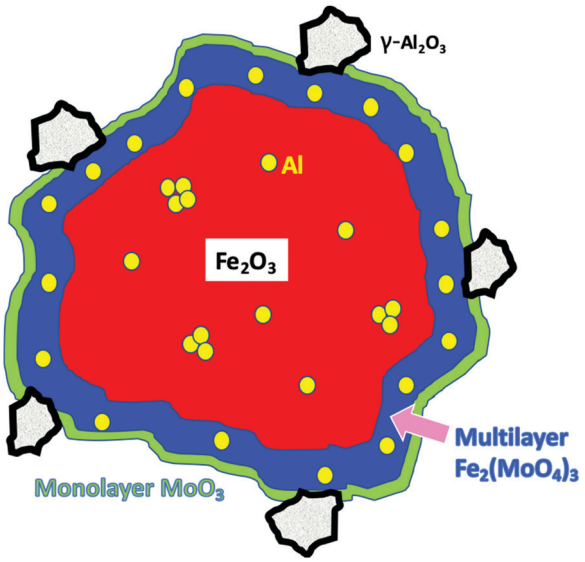

Fig. 11 A schematic model of the Mo coated HAS catalyst with loading of Al.

and CO/CO_2 evolution at higher temperatures, and, as shown in Fig. 11, we propose that this is due to separate alumina (since the desorption looks very much like that from alumina[19]), while there is still a molybdena like layer, which produces formaldehyde. The structure of such materials is further summarised in Fig. 11 and Fig. S9 (ESI†). Fig. 11 shows the situation with high Al loading with Al doping present in several forms, isolated Al oxide (α-like) form, nanoclusters in the bulk (γ-alumina like) and γ-alumina nanoparticles (but still not visible to XRD). When 3 monolayers equivalent of Mo are deposited on the surface, and after calcination, then we have surface layers which contain Mo. The outer layer is MoO_3-like, showing formaldehyde production, with high selectivity, particularly at low temperatures of reaction, while under that there are layers of ferric molybdate [$Fe_2(MoO_4)$], which are partially doped with Al.

Conflicts of interest

There are no conflicts to declare.

Acknowledgements

We are grateful to Diamond Light Source for a part studentship to PH and for support from the UK Catalysis Hub, funded through EPSRC grants EP/I038748/1 and EP/K014714/1, and to the Research Complex at Harwell (RCaH) for the provision of facilities. We thank the Swiss Light Source (SLS) for provision of beamtime under award number 20181979.

References

1 U. Schwertmann, *Soil Sci.*, 1979, **128**, 195–200.
2 U. Schwertmann, R. Fitzpatrick, R. Taylor and D. Lewis, *Clays Clay Miner.*, 1979, **27**, 105–112.
3 D. Bersani, P. P. Lottici and X. Z. Ding, *Appl. Phys. Lett.*, 1998, **72**, 73–75.
4 A. Zoppi, C. Lofrumento, E. M. Castellucci and P. Sciau, *J. Raman Spectrosc.*, 2008, **39**, 40–46.
5 U. Schwertmann and R. M. Cornell, *Iron Oxides in the Laboratory*, John Wiley & Sons, Ltd, 2007, ch. 10, pp. 121–135.
6 S. Chapman, C. Brookes, M. Bowker, E. K. Gibson and P. P. Wells, *Faraday Discuss.*, 2016, **188**, 115–129.
7 W. Li, X. Liang, P. An, X. Feng, W. Tan, G. Qiu, H. Yin and F. Liu, *Sci. Rep.*, 2016, **6**, 35960.
8 A. Andersson, J. Holmberg and R. Häggblad, Process Improvements in Methanol Oxidation to Formaldehyde: Application and Catalyst Development, *Top. Catal.*, 2016, **59**, 1589–1599.
9 A. P. V. Soares, M. F. Portela and A. Kiennemann, *Catal. Rev.*, 2005, **47**, 125–174.
10 M. Bowker, R. Holroyd, A. Elliott, P. Morrall, A. Alouche, C. Entwistle and A. Toerncrona, *Catal. Lett.*, 2002, **83**, 165–176.
11 M. P. House, A. F. Carley and M. Bowker, *J. Catal.*, 2007, **252**, 88–96.
12 M. P. House, M. D. Shannon and M. Bowker, *Catal. Lett.*, 2008, **122**, 210–213.
13 M. P. House, A. F. Carley, R. Echeverria-Valda and M. Bowker, *J. Phys. Chem. C*, 2008, **112**, 4333–4341.
14 C. Brookes, M. Bowker and P. P. Wells, *Catalysts*, 2016, **6**, 92.
15 C. Brookes, P. P. Wells, G. Cibin, N. Dimitratos, W. Jones, D. J. Morgan and M. Bowker, *ACS Catal.*, 2014, **4**, 243–250.
16 M. Bowker, C. Brookes, A. F. Carley, M. P. House, M. Kosif, G. Sankar, I. Wawata, P. P. Wells and P. Yaseneva, *Phys. Chem. Chem. Phys.*, 2013, **15**, 12056–12067.
17 C. Brookes, P. P. Wells, N. Dimitratos, W. Jones, E. K. Gibson, D. J. Morgan, G. Cibin, C. Nicklin, D. Mora-Fonz, D. O. Scanlon, C. R. A. Catlow and M. Bowker, *J. Phys. Chem. C*, 2014, **118**, 26155–26161.
18 M. Bowker, E. K. Gibson, I. P. Silverwood and C. Brookes, *Faraday Discuss.*, 2016, **188**, 387.
19 S. Akarmazyan, P. Panagiotopoulo, A. Kambolis, C. Papadopolou and D. Kondarides, *Appl. Catal., B*, 2014, **145**, 136–148.
20 D. Manuel, D. Cabaret, C. Brouder, P. Sainctavit, A. Bordage and N. Trcera, Experimental evidence of thermal fluctuations on the X-ray absorption near-edge structure at the aluminum K edge, *Phys. Rev. B: Condens. Matter Mater. Phys.*, 2012, **85**, 224108.
21 D. Cabaret and C. Brouder, Origin of the pre-edge structure at the AlK-edge: The role of atomic vibrations, *J. Phys.: Conf. Ser.*, 2009, **190**, 12003.
22 M. Ducher, M. Blanchard, D. Vantelon, R. Nemausat and D. Cabaret, Probing the local environment of substitutional Al^{3+} in goethite using X-ray absorption spectroscopy and first-principles calculations, *Phys. Chem. Miner.*, 2016, **43**, 217–227.
23 M.-A. Arrio, S. Rossano, C. Brouder, L. Galoisy and G. Calas, Calculation of multipole transitions at the FeKpre-edge throughp-dhybridization in the Ligand Field Multiplet model, *Europhys. Lett.*, 2000, **51**, 454–460.

This journal is © the Owner Societies 2020